João Lucas Eberl Simon

A VARIABILIDADE DA FRENTE SUBANTÁRTICA E DO JATO ATMOSFÉRICO NO HEMISFÉRIO SUL

Dissertação submetida ao Programa de Pós-Graduação em Oceanografia da Universidade Federal de Santa Catarina para a obtenção do Grau de Mestre em Oceanografia
Orientadora: Prof.ª Dr.ª Regina R. Rodrigues

Florianópolis
2019

Ficha de identificação da obra elaborada pelo autor,
através do Programa de Geração Automática da Biblioteca Universitária da UFSC.

Simon, Joao Lucas Eberl
A variabilidade da Frente Subantártica e do Jato Atmosférico no Hemisfério Sul / Joao Lucas Eberl Simon ; orientadora, Regina Rodrigues Rodrigues, 2019.
51 p.

Dissertação (mestrado) - Universidade Federal de Santa Catarina, Centro de Ciências Físicas e Matemáticas, Programa de Pós-Graduação em Oceanografia, Florianópolis, 2019.

Inclui referências.

1. Oceanografia. 2. Corrente Circumpolar Antártica. 3. Jato Atmosférico. 4. Circulação Global, Clima. I. Rodrigues, Regina Rodrigues. II. Universidade Federal de Santa Catarina. Programa de Pós-Graduação em Oceanografia. III. Título.

João Lucas Eberl Simon

A VARIABILIDADE DA FRENTE SUBANTÁRTICA E DO JATO ATMOSFÉRICO DO HEMISFÉRIO SUL

Esta Dissertação foi julgada adequada para obtenção do Título de "Mestre em Oceanografia" e aprovada em sua forma final pelo Programa de Pós-Graduação em Oceanografia
Local, 26 de março de 2019.

Prof. Antônio Henrique da Fontoura Klein, Dr.
Coordenador do Curso

Banca Examinadora:

Prof.ª Regina Rodrigues Rodrigues, Dr.ª
Orientadora
Universidade Federal de Santa Catarina

Prof. Carlos Alberto Eiras Garcia, Dr.
Universidade Federal de Santa Catarina

Prof.ª Marina Hirota Magalhães, Dr.ª
Universidade Federal de Santa Catarina

“We're all ghosts driving a
meat-coated skeleton made
from stardust, riding a
rock, hurtling through
space... Fear nothing!”
- unknown

AGRADECIMENTOS

Gostaria de agradecer aos meus familiares por todo o apoio que me deram na jornada até a conclusão deste curso de Pós Graduação. Pois sem eles nada disso seria possível.

Agradeço à minha orientadora profª Regina R. Rodrigues, pelo voto de confiança e pelo apoio até este momento. Sem sua presença me norteando esse trabalho jamais estaria concluído. Agradeço imensamente por todas as horas gastas comigo.

Aos membros da banca meus sinceros agradecimentos. Seu tempo e dedicação certamente melhorarão a qualidade deste trabalho. Vocês terão o poder de me julgar mestre. Uma tarefa talvez já muitas vezes repitida pra vocês, mas um enorme passo para mim. Obrigado por estarem presentes.

Ainda, agradeço aos membros do Programa de Pós-Graduação em Oceanografia da UFSC pois sem seu trabalho e esforço a criação e manutenção deste programa não seria possível.

RESUMO

As variações latitudinais da Frente Subantártica (FSA) e do Jato Troposférico do Hemisfério Sul (JT) são investigados para o período de 1993-2016. Dados de velocidade zonal do vento, altura da superfície do mar e temperatura foram utilizados para identificar essas feições individualmente sobre os oceanos Atlântico Sul, Pacífico Sul e Índico. Durante este período, o jato atmosférico migrou para o polo 0.34°S decada^{-1} no Atlântico, 0.28°S decada^{-1} no Pacífico e 0.14°S decada^{-1} no Oceano Índico. Estudos prévios mostraram que a tendência de migração é devida à expansão do cinturão tropical como consequência do aumento de gases de efeito estufa e resfriamento da estratosfera polar devido à depleção de ozônio. O JT teve um fortalecimento em todas as bacias oceânicas. A FSA representa o limite norte da Corrente Circumpolar Antártica e observou-se na posição média de 46.3°S (±0.5°) no Atlântico, 54.3°S (±0.3°) no Pacífico e 46.6°S (±0.5°) no Índico. A FSA mostrou uma migração sul de 0.46°S decada^{-1} no Atlântico, 0.20°S decada^{-1} no Pacífico e 0.27°S decada^{-1} no Oceano Índico, que é atribuída ao aumento do nível do mar no Hemisfério Sul devido à expansão térmica. A tendência de migração da FSA é consistente com a tendência positiva do Módo Anular Sul no mesmo período. A posição do jato é estatisticamente correlacionada com a posição da FSA. Entretanto os coeficientes de correlação são fracos: +0.22 para o Atlântico, +0.17 para o Pacífico e +0.21 para o Oceano Índico. O deslocamento latitudinal da FSA no Pacífico é inversamente proporcional ao sinal do El Niño – Oscilação Sul (ENSO). Durante anos de El Niño a FSA tende a ter uma posição mais próxima ao polo e durante anos de La Niña mais ao equador, com uma correlação máxima de 0.56 com o ENSO liderando por três meses.

Palavras-chave: Jato Atmosférico, Frente Subantártica, Hemisfério Sul.
.

ABSTRACT

The latitudinal variations of the Subantarctic Front (SAF) and Southern Hemisphere atmospheric jet were investigated for the period of 1993-2016. Zonal wind velocity, sea surface height and temperature data were used to identify these features over the South Atlantic, South Pacific and Indian Oceans individually. During this period, the atmospheric jet migrated poleward 0.34°S decade^{-1} in the Atlantic, 0.28°S decade^{-1} in the Pacific and 0.14°S decade^{-1} in the Indian oceans. Previous works have shown that the poleward trend is due to the expansion of the tropical belt as a consequence of greenhouse gas increase and cooling of polar stratosphere due to ozone depletion. In addition the atmospheric jet strengthen in all three basins. The SAF represents the Antarctic Circumpolar Current northern boundary and was observed in average at 46.3°S (±0.5°) in the Atlantic, 54.3°S (±0.3°) in the Pacific and 46.6°S (±0.5°) in Indian Oceans. The SAF shows a poleward migration of 0.46°S decade^{-1} in the Atlantic, 0.20°S decade^{-1} in the Pacific and 0.27°S decade^{-1} in the Indian Oceans, which is attributed to the sea level increasing in the Southern Hemisphere due to thermal expansion. The SAF poleward trend is consistent with the positive trend of the Southern Annular Mode during the studied period. Moreover, the jet position is statistically significant correlated to the SAF position in each ocean basin. However, the coefficients are weak: +0.22 for the Atlantic, +0.17 for the Pacific and +0.21 for the Indian oceans. The latitudinal displacement of the SAF in the Pacific is inversely proportional to the El Niño-Southern Oscillations (ENSO). During El Niño years the SAF tend to be more poleward and during La Niña years more equatorward, with maximum correlation of 0.56, with ENSO leading by three months.

Descriptors: Subantarctic Front, Atmospheric Jet, Southern Hemisphere.

SUMÁRIO

LISTA DE FIGURAS DA INTRODUÇÃO

LISTA DE ABREVIATURAS E SIGLAS

JT – Jato Troposférico
ASM - Altura da Superfície do mar (ASM)
CCA - Corrente Circumpolar Antártica (CCA)
FP - Frente Polar (FP)
FSA - Frente Subantártica (FSA)

AVISO - *Archiving, Validation, and Interpretation of Satellite Oceanographic data*
DUACS - *Developing Use of Altimetry for Climate Studies*
ECMWF - *European Centre for Medium-Range Weather Forecasts*
ENSO – *El Niño Southern Oscillation*
GIS - *Geographic Information System*
GOCE - *Gravity and Ocean Circulation Experiment*
GODAE - *Global Ocean Data Assimilation Experiment*

11 INTRODUÇÃO

A circulação de larga escala no Hemisfério Sul tem duas feições principais que influenciam grandemente seu clima. Essas feições são conhecidas como a Corrente Circumpolar Antártica (CCA) no oceano e o Jato Troposférico (JT) na atmosfera (Hansen et al. 1984; Toggweiler and Russell 2008; Eichelberger and Hartmann, 2007).

Jatos Atmosféricos são cinturões de fortes ventos de oeste que circulam o globo no nível troposférico da atmosfera em ambos os hemisférios, geralmente localizados em latitudes médias. Eles são formados pela deflexão dos ventos de oeste causada pelo movimento das massas de ar da camada superior da célula de Hadley em direção sul, que causam um fluxo de ar oeste sobre latitudes médias no limite sul da célula, como pode ser observado no esquema da Figura 1. Jatos também são formados por vórtices transientes, que são gerados pelo intenso gradiente termal entre ventos tropicais e polares (Holton, 1992; Bluestein, 1993),

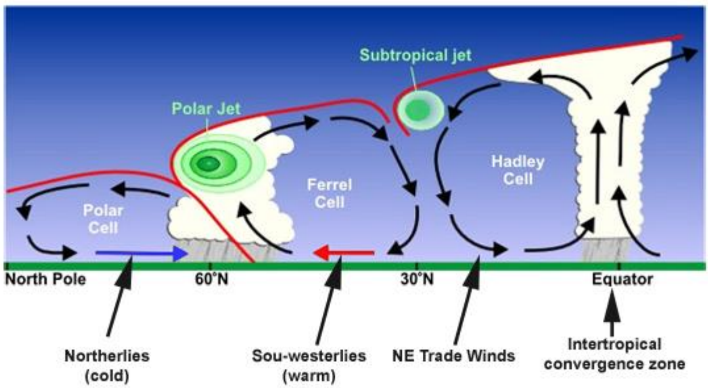

Fonte: NOAA

Figura 1. Seção através da atmosfera no Hemisfério Norte. O ar sobe na zona de convergência intertropical e circula para o norte através da células de Hadley e Ferrel (às vezes separado por um Jato Subtropical fraco) antes de encontrarem o ar frio polar na Frente Polar, onde o Jato Polar está localizado.

O jato é nomeado de acordo com o mecanismo de formação, como Subtropical e Polar, embora estes frequentemente ocupem a mesma região geográfica, tornando a distinção entre eles difícil. Os jatos têm uma importante contribuição para o clima do hemisfério devido à posição de zonas de formação de tempestade estar geralmente ancorada no limite equatorial do jato. Perturbações de escala sinótica são formadas na região de velocidade máxima do vento e migram para menores latitudes trazendo consigo tempestades (Holton, 1992). A presença do jato é caracterizada por fortes ventos, que causam turbulência na região e previnem a formação de furacões, pois os mesmos necessitam de regiões atmosféricas com pouco atrito (Gray, 1968; Vecchi and Soden, 2007). A pequena proporção de continentes no Hemisfério Sul permite um JT contínuo, enquanto no Hemisfério Norte as terras continentais limitam a passagem do jato.

Assim como o JT na atmosfera, a CCA é a maior e mais poderosa corrente oceânica no globo. Tem um transporte de aproximadamente 173 Sv (1 Sv = $\times 10^{6}$ m^{3} s^{-1}; Donohue et al., 2016), contornando o continente antártico. É a única corrente oceânica não limitada pela presença de continentes e é a feição dinâmica dominante do Oceano Austral. Suas águas fazem contato com as porções sul dos oceanos Atlântico, Pacífico e Índico, controlando a temperatura e realizando trocas de nutrientes com os mesmos (Alvain et al. 2008). Também integra o cinturão de convecção global (Conveyor belt), que é responsável pelo ciclo de afundamento e ressurgência de toda a água oceânica (Broecker, 1991).

A corrente é gerada pela diferença de densidade entre as águas das porções norte e sul da CCA, o que causa uma diferença na altura média do nível do mar. Essa diferença gera uma forçante das águas de norte para sul que é compensada pela presença dos ventos de oeste, que mantém essa declividade em equilíbrio dinâmico (Niiler et al., 2003). Sendo assim a corrente é a combinação da circulação de larga escala oceânica e dos fortes ventos de oeste da região (Trenberth et al., 1990; Cunningham et al., 2003).

A posição geográfica da CCA é definida por suas frentes. Frentes são filamentos da corrente que concentram seu transporte de água enquanto ocupam somente ~20% de sua largura (Whitworth et al. 1982). Esses filamentos são zonas de intensa mudança nas propriedades da água, como temperatura e salinidade (Dong et al. 2006), o que causa uma diferença nível do mar entre águas equatoriais e polares devido à expansão termal (Gill, 1982), e um gradiente na distribuição de nutrientes que é altamente limitante para as espécies que habitam a região (Trull et al. 2001), como mostra a figura 2.

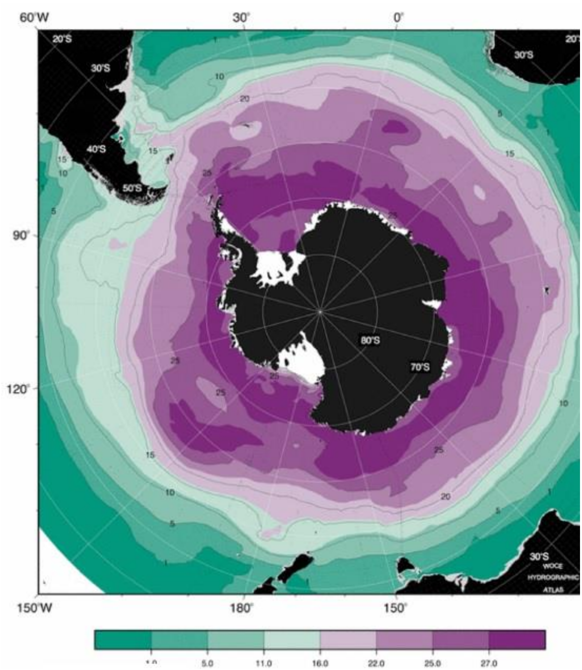

Fonte: Orsi & Whitworth, 2005.

Figura 2. Distribuição de nitrato no Oceano Austral. Os padrões de distribuição de nutrientes são semelhantes à distribuição dos campos de ASM.

Ainda que muitos autores difiram sobre quais frentes melhor representem a CCA e em como localiza-las, a terminologia primeiramente estabelecida por Emery (1977) e revisada por Orsi et al. (1995) separou a CCA, do norte para o sul, como Frente Subantártica (FSA), Frente Polar (FP) e Frente Sul da Corrente Circumpolar Antártica (FSCCA). A FSA é particularmente importante pois é considerada o limite norte da CCA e das águas do Oceano Austral pela Organização Hidrográfica Internacional (1953).

O clima do Hemisfério Sul tem passado por mudanças na última década. A mais notada e documentada é a migração para o polo do JT como consequência da expansão do cinturão tropical devido ao aumento de gases de efeito estufa e pelo resfriamento da estratosfera polar devido à depleção de ozônio (Randel and Wu, 1999; Hu and Fu, 2007; Polvani et al., 2011; Swart and Fyfe 2012; Polvani et al. 2013). Enquanto diversos estudos tiveram enfoque nos ventos do Hemisfério Norte, somente alguns focaram as mudanças nas frentes oceânicas e na CCA.

Gille (2014) Notou uma movimentação dos contornos na altura da superfície do mar (ASM) na região da CCA que eram consistentes com o aquecimento das águas austrais, e por sua vez ameaçam aumentar o derretimento basal em regiões onde a corrente localiza-se mais próxima do continente antártico. (Graham et al., 2012; Pritchard et al., 2012; de Boer et al., 2013). A Figura 3 mostra um esquema da interação entre diversos processos da circulação austral.

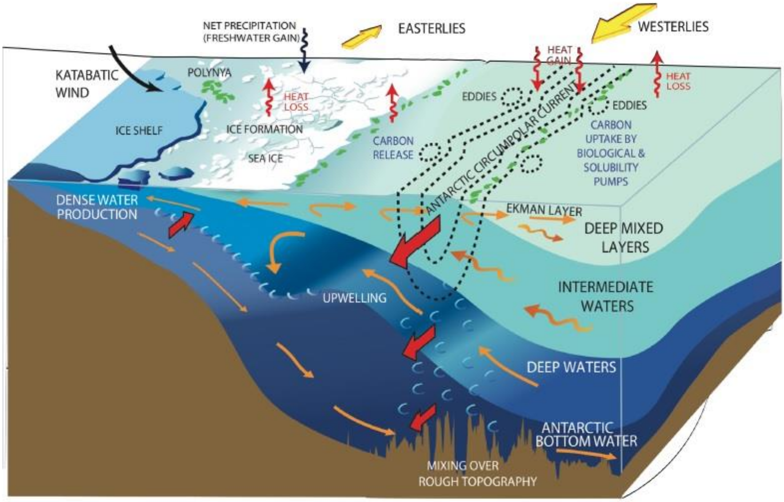

Fonte: National Research Council (2011).

Figura 3. Esquema dos processos ocorrendo na circulação de larga escala do Oceano Austral. Grandes setas vermelhas indicam a direção media do fluxo na Corrente Talude Antártica e na CCA. Setas laranjas indicam a circulação das massas d’água. Setas amarelas indicam a direção dos ventos prevalescentes, e setas vermelhas finas indicam trocas de calor.

Nos últimos 100 anos a média da temperatura global subiu aproximadamente 0.6^{o}C, e é estimado que continue a aumentar numa escala cada vez mais rápida (Houghton et al., 2001). Impactos substanciais já são vistos na produção agrícola (Peng et al., 2004), e diversas espécies sensíveis a mudanças na temperatura estão à margem da extinção (Bustamante et al., 2006).

Baseado na discussão mencionada, o objetivo principal desse estudo é investigar a variação latitudinal do JT e da FSA individualmente nos oceanos Atlântico Sul, Pacífico Sul e Índico. No entanto, tem sido difícil estudar essas feições globais devido à falta de dados *in situ* com cobertura espacial e temporal adequada, principalmente em regiões oceânicas. Recentemente satélites vêm provendo dados de alta resolução temporal e espacial, além de cobertura global, permitindo estudos mais detalhados da localização das correntes oceânicas e frentes (Belkin & O'Reilly, 2009; Sokolov & Rintoul, 2007), ainda que sensoriamento remoto sofra com a falta de validação dos dados com amostras *in situ*.

Novos métodos de coleta de dados hidrográficos que consomem menos tempo e recursos tem surgido, como flutuadores que coletam dados à medida que são carregados pelas correntes. O programa Argo é a maior fonte atual de dados de flutuadores, amostrando verticalmente a coluna d'água e coletando dados de temperatura, salinidade e pressão desde 1997 (Roemmich & Gilson, 2009). O crescente banco de dados dos flutuadores pode ser usado para identificar correntes oceânicas e frentes (Giglio & Johnson, 2015), mesmo não tendo a mesma resolução temporal dos dados satelitais (Kim & Orsi, 2014).

O segundo objetivo deste estudo é desenvolver uma metodologia de identificação da posição da FSA combinando dados de satélite e de flutuadores. Durante a fase de resultados, ao investigar a variação latitudinal da FSA no Pacífico constatou-se que o sinal era diferente das demais bacias oceânicas, suspeitando-se influência de oscilações de baixa frequência como o El Niño – Oscilação Sul (ENSO). O El Niño é parte de um padrão climático que ocorre quando a temperatura da superfície do Oceano Pacífico tropical aumente acima da média por um período de tempo extenso. Seu oposto é a fase de La Niña (negativa), onde a temperatura do Pacífico central diminuí abaixo da média (Byrne, 2019). O NINO é um índice que mede a intensidade da passagem de El Niños e La Niñas e é calculado pela média da temperatura da superfície do mar em diferentes regiões do Pacífico Tropical, como mostra a Figura 4.

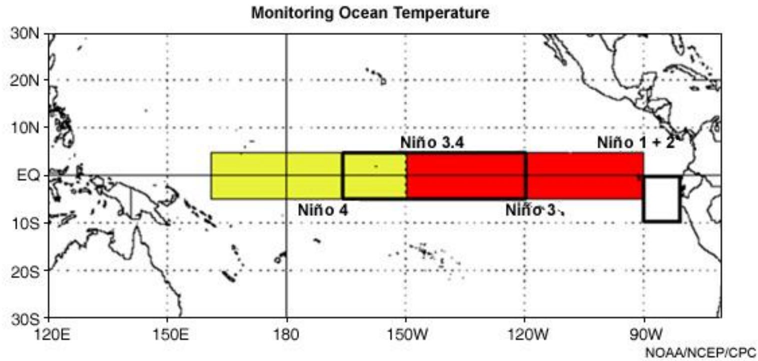

Fonte: NOAA

Figura 4. Diferentes regiões onde é medida a temperature para gerar os índices ENSO.

Assim, como objetivo adicional, este estudo comparou o índice do ENSO – NINO 3.4 com as variações latitudinais da FSA no Oceano Pacífico, após seu sinal ter sido filtrado de oscilações de alta frequência e interanuais, para verificar uma relação entre os sinais.

2 JUSTIFICATIVA

Nos últimos anos tem-se observado diversas mudanças no clima global que, apesar de ainda não terem influência direta sobre a vida humana, já começam a ameaçar a sobrevivência de diversas outras espécies. Investigar como importantes feições da circulação global têm respondido a essas mudanças é imperativo para conhecermos o grau de impacto que elas irão exercer no futuro, bem como entender sua extensão. A posição geográfica dessas feições é influenciada por diversos fatores climáticos, de modo que esse trabalho se justifica ao investigar como a posição geográfica dessas feições mudou nos últimos anos, podendo inferir informações sobre o clima global.

3 OBJETIVOS

3.1 Objetivo Geral

1.1

O objetivo principal desse estudo é investigar a variação latitudinal do JT e da FSA individualmente nos oceanos Atlântico Sul, Pacífico Sul e Índico entre o período de 1993-2016.

3.2 Objetivos Específicos

(1) Mapear a posição do JT utilizando dados de velocidade zonal do vento para o período estudado.

(2) Desenvolver uma metodologia de identificação da posição da FSA combinando dados de satélite e de flutuadores Argo.

(3) Investigar tendências nas séries temporais.

(4) Comparar o índice ENSO – NINO 3.4 com as variações latitudinais da FSA no Oceano Pacífico, após seu sinal ter sido filtrado de oscilações de alta frequência e interanuais, para verificar correlações.

4. HIPÓTESE

Serão testadas as seguintes hipóteses:

1. Se existe uma relação entre a posição geográfica do JT e da FSA no Hemisfério Sul.

2. Se há diferenças na taxa de migração observada nas feições dinâmicas para cada bacia oceânica.

3. Se é possível detectar a influência do ENSO na FSA no Oceano Pacífico Sul.

THE VARIABILITY OF THE SUBANTARCTIC FRONT AND THE SOUTHERN HEMISPHERE ATMOSPHERIC JET

Este capítulo apresenta o conteúdo do artigo que compõe esta dissertação e foi submetido à revista *Brazilian Journal of Oceanography* em 06/03/2019. O conteúdo apresentado a seguir segue na íntegra o submetido na revista, mudando apenas a formatação do texto. A confirmação da submissão é apresentada na próxima página.

Submitted Article - Brazilian Journal of Oceanography

Braz. j. oceanogr. - GNPapers <gnpapers@gnpapers.com.br>
Qua, 06/03/2019 14:28
Para: Joao Lucas Eberl Simon <jl.simon@hotmail.com>

BRAZILIAN JOURNAL OF OCEANOGRAPHY

Dear Sir (Madam)
Dr. Joao Lucas Eberl Simon

Article Number: 256
Section: Full Articles

We inform that the article "The variability of the subantarctic front and the Southern Hemisphere atmospheric jet" was received. It'll be sent to review for possible publication in Brazilian Journal of Oceanography. Please, for future communication about the article use the article number above.

The Authors declare that the manuscript consists entirely of an original work and it isn't being under consideration by another Brazilian of foreigner publication, or it isn't being considered for publication elsewhere in any format and/or media (printed or electronic).

Thanks for submitting to us your article.

Sincerely,

Prof. Dr. Rubens Mendes Lopes
Editor-in-chief

««« Sent by GNPapers - This is an automated message - Please do not reply directly to this email »»»

THE VARIABILITY OF THE SUBANTARCTIC FRONT AND THE SOUTHERN HEMISPHERE ATMOSPHERIC JET

Running title: Subantarctic front and southern atmospheric jet

João L. E. Simon*, Regina R. Rodrigues

Department of Oceanography, Federal University of Santa Catarina (R. Eng. Agronômico Andrei Cristian Ferreira, s/n - Trindade, Florianópolis - SC, 88040-900)

Corresponding author: jl.simon@hotmail.com

ABSTRACT

The latitudinal variations of the Subantarctic Front (SAF) and Southern Hemisphere atmospheric jet were investigated for the period of 1993-2016. Zonal wind velocity, sea surface height and temperature data were used to identify these features over the South Atlantic, South Pacific and Indian Oceans individually. During this period, the atmospheric jet migrated poleward 0.34°S decade^{-1} in the Atlantic, 0.28°S decade^{-1} in the Pacific and 0.14°S decade^{-1} in the Indian oceans. Previous works have shown that the poleward trend is due to the expansion of the tropical belt as a consequence of greenhouse gas increase and cooling of polar stratosphere due to ozone depletion. In addition the atmospheric jet strengthen in all three basins. The SAF represents the Antarctic Circumpolar Current northern boundary and was observed in average at 46.3°S (±0.5°) in the Atlantic, 54.3°S (±0.3°) in the Pacific and 46.6°S (±0.5°) in Indian Oceans. The SAF shows a poleward migration of 0.46°S decade^{-1} in the Atlantic, 0.20°S decade^{-1} in the Pacific and 0.27°S decade^{-1} in the Indian Oceans, which is attributed to the sea level increasing in the Southern Hemisphere due to thermal expansion. The SAF poleward trend is consistent with the positive trend of the Southern Annular Mode during the studied period. Moreover, the jet position is statistically significant correlated to the SAF position in each ocean basin. However, the coefficients are weak: +0.22 for the Atlantic, +0.17 for the Pacific and +0.21 for the Indian oceans. The latitudinal displacement of the SAF in the Pacific is inversely proportional to the El Niño-Southern Oscillations (ENSO). During El Niño years the SAF tend

to be more poleward and during La Niña years more equatorward, with maximum correlation of 0.56, with ENSO leading by three months.

Descriptors: Subantarctic Front, Atmospheric Jet, Southern Hemisphere.

INTRODUCTION

The large-scale circulation of the Southern Hemisphere has two major features that greatly influence its climate. These features are known as the Antarctic Circumpolar Current (ACC) on the ocean and the Tropospheric Jet Stream (TJS) on the atmosphere (Hansen et al. 1984; Toggweiler and Russell 2008; Eichelberger and Hartmann, 2007). Jet streams are bands of strong westerly winds that circulate the globe at the tropospheric level of the atmosphere in both hemispheres, usually located at mid latitudes. They are formed by the westerly deflection of wind direction caused by the poleward movement of the air masses at the upper level of the Hadley cell, which causes a westerly air flux at the mid latitude end of the cell. Jets are also formed on mid latitude transient eddies by the sharp thermal gradient between warm tropical and cold polar winds (Holton, 1992; Bluestein, 1993). The jets are named by this difference in the formation mechanism, as Subtropical and Polar Jet, although they often occupy the same locations, making the distinction difficult. The jets have an important contribution to the hemisphere's climate as the position of storm tracks is often anchored on the equatorward limit of the jet. Synoptic scale disturbances are formed on the maximum wind speed location and migrate to lower latitude bringing storms along with (Holton, 1992). The presence of jets is characterized by strong winds, which cause turbulence on the jet's region and prevent hurricane formation, as they require low-sheer atmosphere regions (Gray, 1968; Vecchi and Soden, 2007). The small proportion of continents in the Southern Hemisphere allows a continuous TJS, while in the North Hemisphere the landmasses limit the jet's passage.

As the jet stream in the atmosphere, the ACC is the strongest and longest oceanic current in the globe. It has a transport of approximately 173 Sv (1 Sv = $\times 10^6$ m^3 s^{-1}; Donohue et al., 2016), surrounding the Antarctic continent in its full extension. It is the only current not to be limited by the presence of continents and is the dominant dynamic feature of the Southern Ocean. The current is generated by the combination of large-scale oceanic circulation and the strong westerly winds of the region (Trenberth et al., 1990; Cunningham et al., 2003). The geographical position of the ACC is defined by the position of its fronts. Fronts are narrow areas that concentrate the current's water transport while occupying only about 20% of its width (Whitworth et al. 1982). These bands are zones of intense change in water proprieties, such as temperature and salinity (Dong et al. 2006), which causes a difference in the sea level between warm equatorward and cold poleward waters due to thermal expansion (Gill, 1982), and a nutrient gradient that is highly limiting to the species who habitat the region (Trull et al. 2001). Although many authors differ between which fronts better represent the ACC and how to locate them, the terminology first established by Emery (1977) and reviewed by Orsi et al. (1995) separates the ACC as, from north to south, in Subantarctic Front (SAF), Polar Front (PF), and South Antarctic Circumpolar Current Front (SACCF). The SAF is particularly important because is considered the northern limit of the ACC and Southern Ocean waters by the International Hydrographic Organization (1953).

The climate of the Southern Hemisphere has experienced changes in the last decades. The most noticed and documented is the poleward shift of the TJS as a consequence of the expansion of the tropical belt due to the greenhouse gases increase and the cooling of the polar stratosphere due to ozone depletion (Randel and Wu, 1999; Hu and Fu, 2007; Polvani et al., 2011; Swart and Fyfe 2012; Polvani et al. 2013). While several studies have focused on the Southern Hemisphere winds, only a few have focused on the changes of the oceanic fronts and the ACC. For instance, Gille (2014) noticed a poleward displacement in sea surface height contours at the Antarctic Circumpolar Current's region that is consistent with a warming of the southern waters and this in turn may increase basal melting in regions where the current is closer to the Antarctic continent (Graham et al., 2012; Pritchard et al., 2012; de Boer et al., 2013)

Based on the aforementioned discussion the main objective of this study is to investigate the TJS and SAF latitudinal variation on the South Atlantic, Indian and Pacific Oceans individually. However, it has always been challenging to study these global features due to the lack of *in situ* data with spatial and temporal coverage, particularly in the ocean. More recently, satellites have provided higher spatial and temporal resolution data with global coverage allowing more detailed studies of the location of ocean currents and fronts (Belkin & O’Reilly, 2009; Sokolov & Rintoul, 2007). Though, remote sampled data still commonly lacks *in situ* validation of its results. New ways of collecting hydrographic data that are less expensive and timing consuming have advanced such as floats that collect data as they drift. The Argo program is the current biggest float data source, sampling vertically the water column collecting temperature, salinity and pressure data since 1997 (Roemmich & Gilson, 2009). The constantly growing float dataset can be used to identify ocean currents and fronts (Giglio & Johnson, 2015), even though it does not have the same temporal resolution as satellite data (Kim & Orsi, 2014). The second objective of this study is to develop a methodology to identify the position of the SAF combining satellite with float data.

DATA AND METHODS

The data used in this study to compute the latitudinal position of the jet was obtained from the European Centre for Medium-Range Weather Forecasts (ECMWF) ERA-Interim reanalysis for the period of 1993–2016 with a spatial resolution of 0.75°x0.75° (Dee et al. 2011). Daily values are obtained by averaging the 6-hourly zonal wind data. The jet latitudinal position is computed according to Woollings et al. (2010). The zonal wind is first vertically averaged within 4 pressure levels 700 hPa, 775 hPa, 850 hPa and 925 hPa and then zonally averaged over three longitudinal sectors, the Atlantic sector (67°E – 20°W), Pacific sector (146°W – 67°E) and Indian sector (20°W – 146°W), neglecting winds above 80°S and under 10°S. The resulting zonal wind data are filtered by applying a low-pass 10-day Lanczos filter with a 61-day window (Duchon, 1979) to avoid high-frequency disturbances. The daily latitudinal position of the jet is then computed as the latitude of the maximum zonal wind (Figure 1) for each sector.

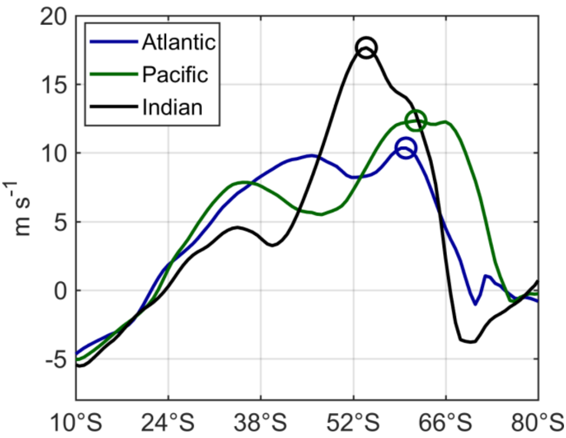

Figure 1. Zonally averaged wind speed (m s^{-1}) after applying the Lanczos filter for the period of 1993-2016. The circles indicate the jet latitudinal position.

The Subantarctic Front defines the ACC northern limit. To find its position the contour-based method was employed using Sea Surface Height (SSH) data (Thompson & Sallee, 2012; Sallee et al. 2008; Orsi et al. 1995; Graham et al. 2012; Sokolov & Rintoul, 2009a). The absolute dynamic topography data, treated here as SSH, was obtained by the Developing Use of Altimetry for Climate Studies (DUACS) and formerly distributed by Archiving, Validation, and Interpretation of Satellite Oceanographic data (AVISO), being made available now by the Copernicus Marine Environment Monitoring System (CMEMS, 2018). The data covers the period of 1993-2016 and was daily sampled with a spatial resolution of 0.25°×0.25°. We use a methodology by Kim & Orsi (2014) to determine the SSH contour that best fits the SAF position for Scotia Sea region (40°S-65°S, 70°W-40°W) for each time step using additional high quality hydrographic profiles (Figure 2). The hydrographic data were obtained from 20,022 profiles sampled within the Scotia Sea limits for the period of 2010-2017 by the International Argo Program, and distributed by the Global Ocean Data Assimilation Experiment (GODAE; Argo, 2000). The depth of sampling was calculated from the pressure and latitudinal position of each profile using UNESCO algorithm (Fofonoff and Millard, 1983). Only profiles flagged as good data by the Argo flag system (Argo, 2017) were used. The profile data was linearly interpolated and checked with Pearson's correlation (Benesty et al. 2009), filtering out profiles that had a correlation lower than 90% ($p<0.05$) with the original data. The interpolation set the vertical resolution of the temperature profiles to 1 meter and discarded samples shallower than 15m or deeper than 1000 m, only generating data between the first and last pressure levels sampled by each float. The area around Drake Passage was chosen to use the Argo floats to determine the SAF position due to its topography features. The bottleneck effect in this area limits the ACC position (Grahan et al. 2012) and forces the SAF to go north along the South America continental slope (Cunningham et al. 2003).

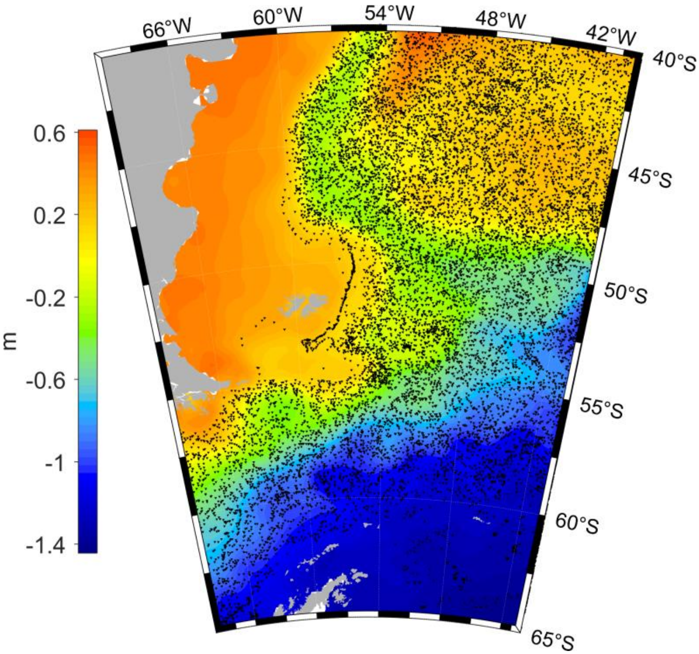

Figure 2. Sea surface height (m) averaged over the Scotia Sea region and for the period of 1993- 2016. The black dots represent the position of 20,022 Argo profiles from 2010 to 2017.

The daily SSH gridded data were time averaged and then zonally averaged along the longitudinal section for each ocean basin (Figure 3). The temperature profiles from Argo were grouped by year and averaged for the same grid boxes from the SSH data. This procedure was done for each depth level separately. The resulting temperature gridded data were zonally averaged within the Scotia Sea limits, then time averaged over the data period (Figure 4). Finally, the temperature data was vertically averaged (Figure 5) and compared with the zonally averaged SSH to find the northernmost region of fast declining on both SSH and temperature, which was accomplished by calculating the anomaly of the series and extracting the one dimension gradient. The temperature gradient was smoothed with a moving-average filter of 1.25° window, and the latitudinal position of the northern peak in both gradients was extracted and used to find the corresponding value on the averaged SSH profile of the Scotia Sea.

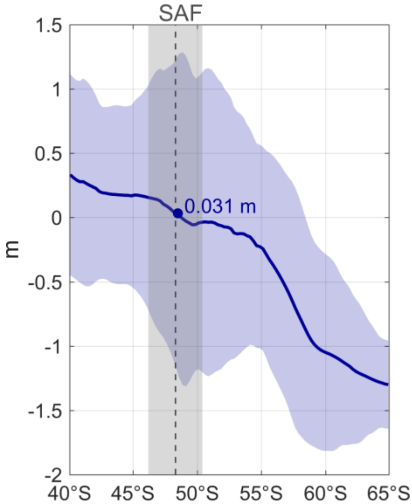

Figure 3. SSH (m, solid blue) averaged over the Scotia Sea area for the period of 1993-2016. Area shaded in blue shows the local standard deviation and in grey the SAF, dashed line shows the peak of the gradient.

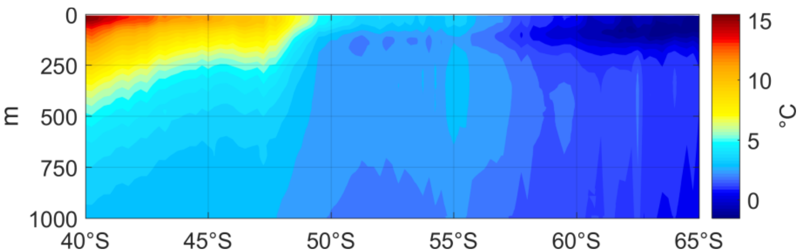

Figure 4. Zonal mean temperature (°C) from Argo profiles averaged for the Scotia Sea region (40°S-65°S, 70°W-40°W) and for the period of 2010-2017.

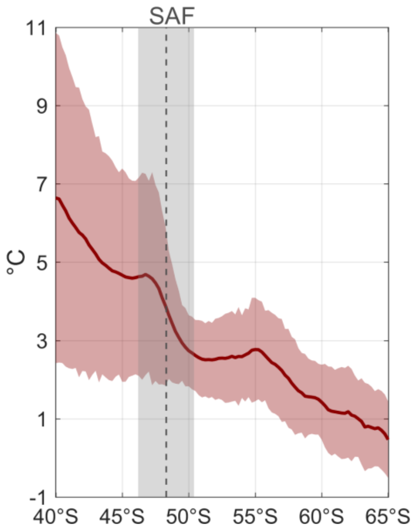

Figure 5. Temperature (°C) from Argo data (solid red) averaged over the Scotia Sea area and for the period of 2010-2017. Area shaded in red shows the local standard deviation and in grey the SAF, dashed line shows the peak of the gradient.

The gradient profiles evidenced the two major transition sections, observed around 48°S and 57°S (Figure 6). The northern peak exhibited the highest temperature contrast between northern and southern portions, as well as the second highest contrast in SSH, evidenced in the gray areas of Figures 3 and 5. The latitudinal position of these peaks (circled in red and blue) was used to find the associated SSH value, demonstrated by the intersection between dashed line and the SSH profile. The SSH value of 0.031m was used for the front location on a global scale by drawing isometric contour lines in the daily SSH grids and filtering to retain only continuous lines surrounding the globe, which excluded false positives caused by interactions with rings. The latitudinal position of the remaining contour lines was extracted and reorganized in the original grid spatial resolution of 0.25°x0.25°. The SAF daily position was obtained by verifying the gridded latitudinal interval most frequently occupied by the contour line in each ocean basin. Once the daily latitudinal position of both SAF and TJS were obtained for each sector, a linear trend was fitted to the data using the minimum least square method (Chatterjee et al., 2000) to verify any trend on the series.

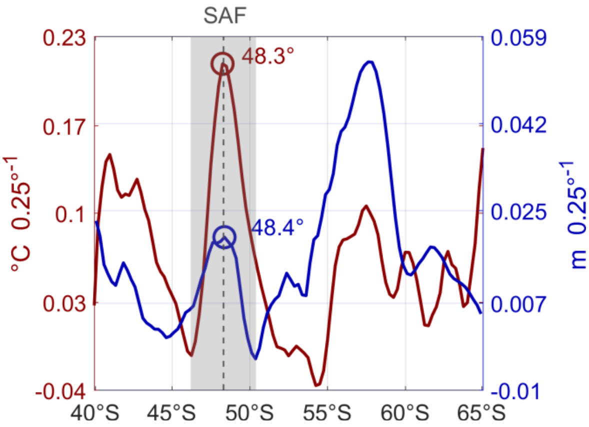

Figure 6. Gradients of sea temperature (°C, red) and sea surface height (m, blue) in Scotia Sea. Shaded gray area represents SAF and dashed line shows the peak in the gradient (circles).

To investigate the link between ENSO and SAF we use monthly NIINO3.4 data obtained from the Global Climate Observing System (GCOS) Working Group on Surface Pressure (WG-SP) for the period of 1993-2016 (Trenberth & Stepaniak, 2001). A Fourier analysis (Bracewell, 1966) was performed to extract the seasonal cycle from the SAF latitudinal position time series. Then, the SAF latitudinal position time series for the Pacific basin were detrended to performer the correlation analysis with the jet position and ENSO index.

RESULTS

The averaged zonal wind is presented in Figure 7. As expected, the higher velocities are concentrated in a belt between 40°S and 60°S surrounding the Antarctic continent. The Andes Mountain Range strongly limits the jet passage, forcing its pattern poleward on the southern region of South America. The highest wind speeds were found over the Indian Ocean, with an average of 13.0 m s^{-1} (±2.17). The Atlantic and Pacific present averaged winds of 11.0 m s^{-1} (±1.88) and 9.93 m s^{-1} (±2.09). The averaged jet latitudinal position was at 49.8°S (± 6.22) in the Atlantic, 54.2°S (± 6.67) in the Pacific and 49.1°S (± 4.13) in the Indian. The TJS latitudinal position is known to be correlated to storm tracks, which are zones of cyclogenesis and storm formation that impact the climate on the Southern Hemisphere (Trenberth, 1991). The cyclone development on the Southern Hemisphere starts to happen between 35°S and 55°S, exhibiting mature systems between 40°S and 60°S (Carleton, 1979). The jet's position found in this study supports this claim, with the average position ~50°S in the Atlantic and Indian sectors and ~55°S in the Pacific (Figure 7). This ~5° difference in the jet's core latitudinal position between ocean basins was also observed by Trenberth et al. (1990). The jet core latitudinal position in each basin remains close to the observed by Nakamura and Shimpo (2004) and by Archer and Caldera (2008).

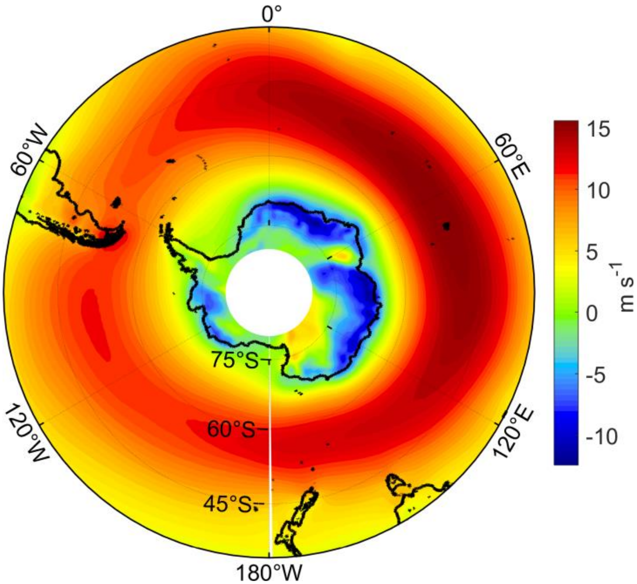

Figure 7. Map of zonal wind speed (m s^{-1}) averaged for the period of 1993-2016 and between 700 and 925 hPa. Positive (negative) values represent winds from west (east).

The time series of latitudinal position of the jet over the studied period is shown in Figure 8. Previous studies have already reported a global poleward shift of the jet (Randel and Wu, 1999; Hu and Fu, 2007; Polvani et al., 2011; Swart and Fyfe 2012; Polvani et al. 2013). Our study investigates this migration individually for the three ocean basins. As for the global case, there is a negative trend (poleward shift) in all three ocean basins that are statistically significant, except for the Indian Ocean (Table 1). If one considers the trends for the period of 2000-2016, they are higher and statistically significant for all three ocean basins, but reverses the sign in the Pacific. This is probably due to the Interdecadal Pacific Oscillation (IPO) that reversed its sign from positive to negative in 2000, when the trade winds strengthening over the tropical Atlantic (England et al., 2014) and the tropical Pacific became cooler with more La Niñas. This is consistent with the idea that the expansion of the tropical belt due to global warming pushes the jet poleward but in the case of Pacific pushes the jet equatorward associated with cooling due to the natural variability of the IPO.

Table 1. Trends per decade for the jet latitude, maximum jet velocity and SAF latitude. Trends statistically significant at 95% confidence level are displayed in bold using the nonparametric Mann-Kendall test.

Trend (per decade)	1993-2016	2000-2016
South Atlantic Jet Latitude	**-0.34°**	**-0.55°**
South Pacific Jet Latitude	**-0.28°**	**+1.41°**
South Indian Jet Latitude	-0.14°	**-1.42°**
South Atlantic Jet Intensity	**+0.22 m/s**	+0.02 m/s
South Pacific Jet Intensity	**+0.34 m/s**	**-0.67 m/s**
South Indian Jet Intensity	**+0.14 m/s**	**+0.37 m/s**
South Atlantic SAF Latitude	**-0.46°**	**-0.28°**
South Pacific SAF Latitude	**-0.20°**	**-0.12°**
South Indian SAF Latitude	**-0.27°**	**-0.19°**

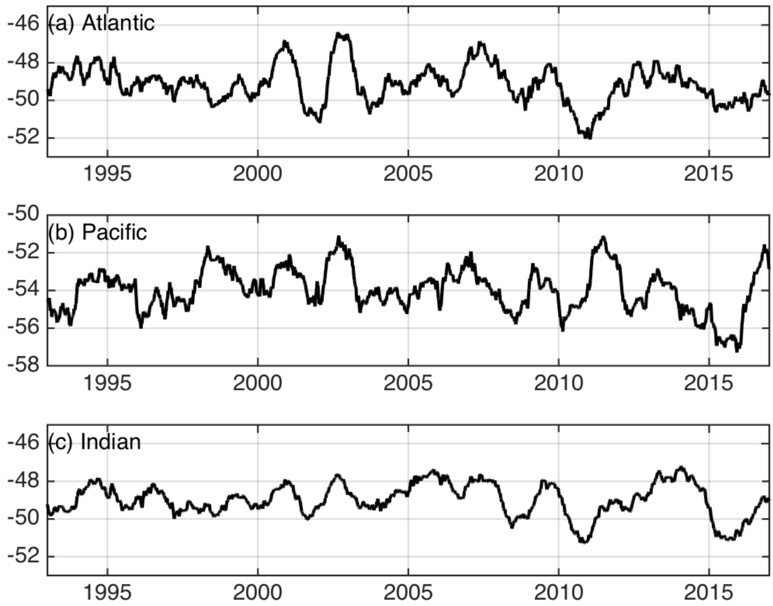

Figure 8. Time series of the jet latitudinal position (°) for (a) Atlantic, (b) Pacific and (c) Indian oceans.

The time series of maximum zonal velocity along the jet core is also computed and shown in Figure 9. Corroborated by the same previous studies, there is an intensification of the jet in all three ocean basins with the trends statistically significant (Table 1). Again when the trends are computed for the period of 2000-2016, there is a weakening of the jet over the Pacific due to the cooling of the tropical Pacific associated with negative phase of the IPO. This is consistent with the fact that the jet is a response to the meridional temperature gradient between the tropics and midlatidudes. The cooling of the Pacific weakens the temperature gradient and thus the jet.

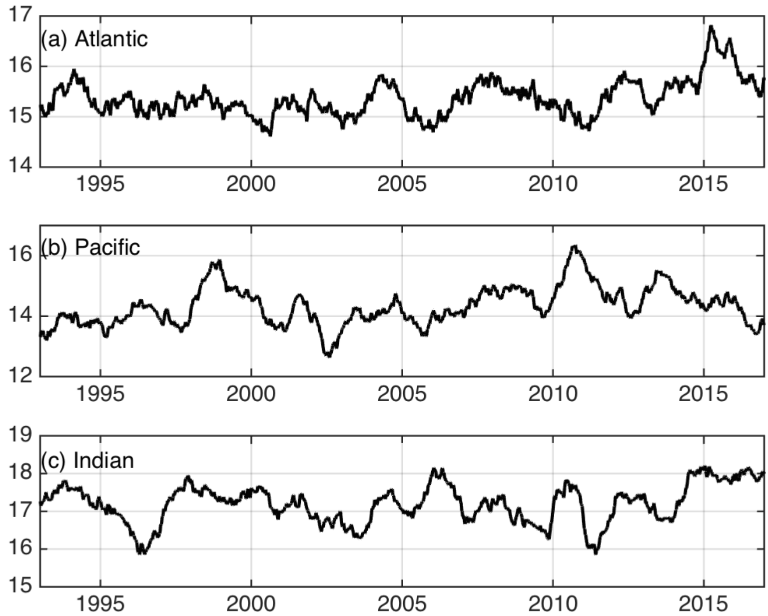

Figure 9. Time series of the maximum zonal velocity (m^{-1} s^{-1}) along the core of the atmospheric jet for (a) Atlantic, (b) Pacific and (c) Indian oceans.

Now we turn our attention to the SAF variability. The time averaged SSH for the period of 1993-2016 is shown in Figure 10. The sea surface height decreases poleward, and it is possible to observe lower heights in regions of colder water currents such as the Falkland Current, as well as higher heights in warmer water current such as the Agulhas Current. The contours follow topography features, and it is possible to notice elevations such as the Campbell Plateau in south New Zealand in the SSH mean map. Previous studies have used SSH data to determine the ACC frontal systems. For instance, applying a contour method on SSH fields, Sokolov and Rintoul (2009b) observe that fronts do not maintain a single-filament structure all around the Antarctic continent, but rather divide in two or more bands and remerge as the topography dictates. Chapman (2014) show, on the other hand, that single band contour applied in cumulative incidence on a global scale has the best noise/signal ratio of the common location methods (gradient method, probability density function method), which explains the similarities between the SAF geographical position found here and in

Sokolov and Rintoul (2007, 2009b). Our results also agree well with Orsi et al. (1995) in the Pacific and Atlantic basins. Around South Australia, our results differs from Orsi et al. (1995) but agrees with Belkin and Gordon (1996), which is a more detailed study between South Africa and Tasmania. Our results are also similar to Sun and Watts (2002), which use a stream function method, for shallower regions such as the Campbell and Kerguelen Plateaus.

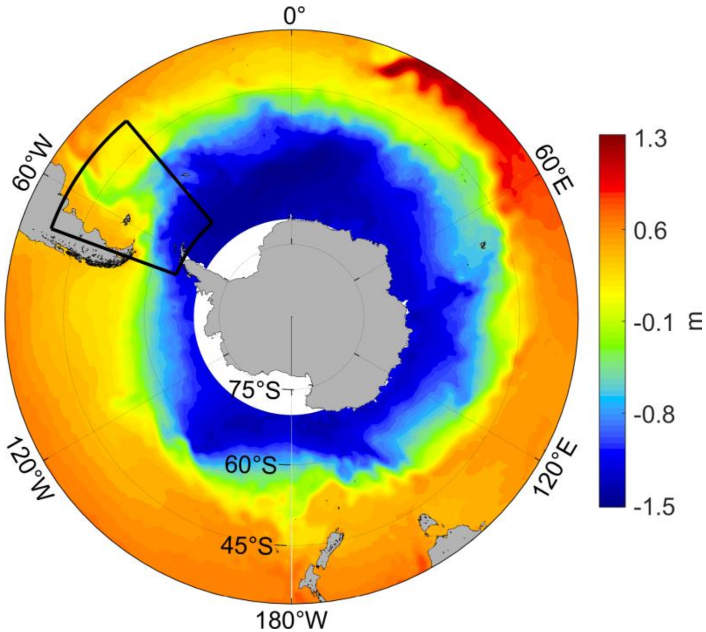

Figure 10. Map of Sea Surface Height (m) averaged for the period of 1993-2016. The black box displays the Scotia Sea area (40°S-65°S, 70°W-40°W) where the methodology with float data was applied.

The SAF local frequency of occurrence reinforced the strong correlation between topography features and the ACC (Figure 11). Regions with shallower depths presented a strong anchorage of the SAF position and consequent high frequency of occurrence, hence the thinner lines (higher frequencies) at the southern South America continental slope. The SAF position is also limited poleward by the Kerguelen's Plateau, and equatorward by the Campbell Plateau. The front exhibited stability as well where it crossed mid-ocean ridges such as the Mid-Atlantic Ridge, Pacific Antarctic Ridge and Southeast Indian Ridge.

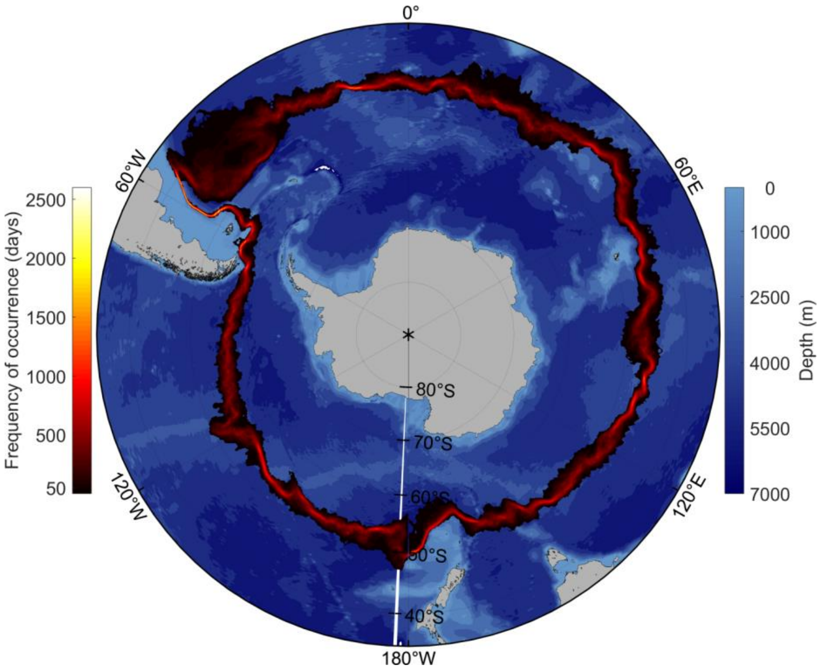

Figure 11. Map of the SAF geographical frequency of occurrence (days) for the period of 1993-2016 over topography.

The time series of the SAF latitudinal position is shown in Figure 12 for the three ocean basins separately. The long-term linear trend shows the decadal poleward migration over the observed period for the Atlantic, Pacific and Indian oceans, however with different rates. The linear trend was -0.46°S decade-1 for the Atlantic, -0.20°S decade-1 for the Pacific and -0.27°S decade-1 for the Indian oceans (Table 1). This is similar to the results for the TSJ. The SAF poleward migration has been observed by Kim and Orsi (2014) and Gille (2014). Gille (2014) focuses on the ACC transport and showed that the transport does not follow the latitudinal migration observed from SSH contours, arguing that this migration may be related to large scale sea surface level changes occurring on the Southern Hemisphere rather than a regional current displacement. Although the SSH may not reflect a migration in the current transport, its geographical location is linked with other water proprieties, such as temperature, nutrients and density. The SAF poleward shift indicates warmer waters reaching farther south in the last decades, which threatens habitats of highly endemic Antarctic species (Trull et al. 2001). For this reason, it is important to monitor the SAF contour, even if does not represents the position of the ACC.

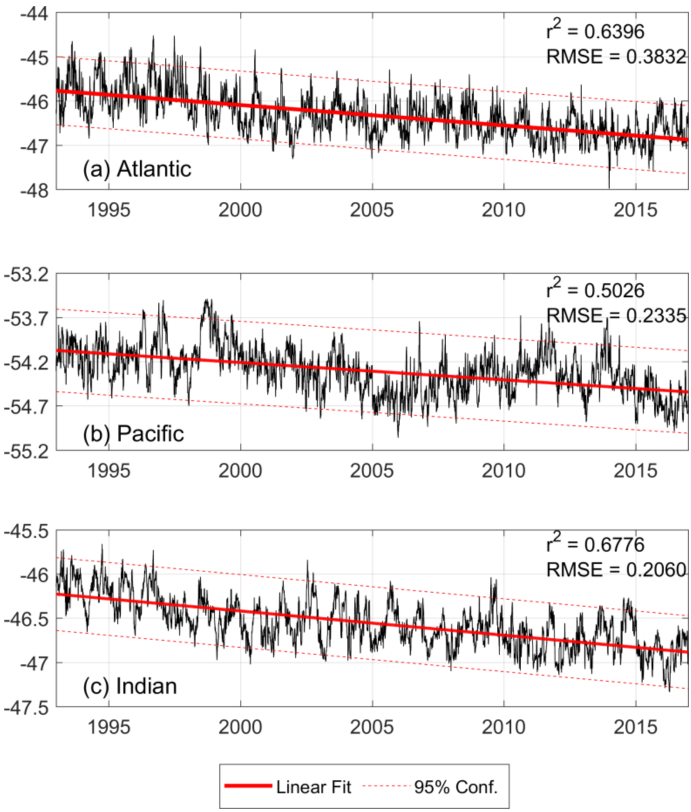

Figure 12. SAF daily (1993-2016) latitudinal position (°), zonally averaged over the (a) Atlantic, (b) Pacific and (c) Indian sectors. Solid red lines represent the best linear fit, with Pearson's correlation (r^2) and Root Mean Squared Error (RMSE) displayed on the top/right. Dashed red lines represent the 95% confidence interval.

As for the TJS, the Pacific SAF shows a different pattern from the other two ocean basins, which motivated a more detailed analysis of the signal to verify if the ENSO/IPO relationship was responsible for such pattern. Figure 13 shows the de-trended SAF latitudinal position for the Pacific and the reconstructed modeled data obtained from a Singular Value Decomposition analysis (Golub & Reinsch, 1970) using the most energetic frequencies found in the Fourier transformation, excluding the seasonal cycle. The reconstructed signal is then plotted against the ENSO index in Figure 14. A lagged cross-correlation analysis between the two series was performed and the maximum correlation of -0.56 occurs with ENSO leading for three months the SAF time series. The negative correlation means that during El Niño years the SAF tend to be more poleward and during La Niña years more equatorward. This is consistent with the jet position. When the tropical Pacific is cooler the jet is more equatorward and so thus the SAF. This result agrees with Sallé et al. (2008) and Kim and Orsi (2014).

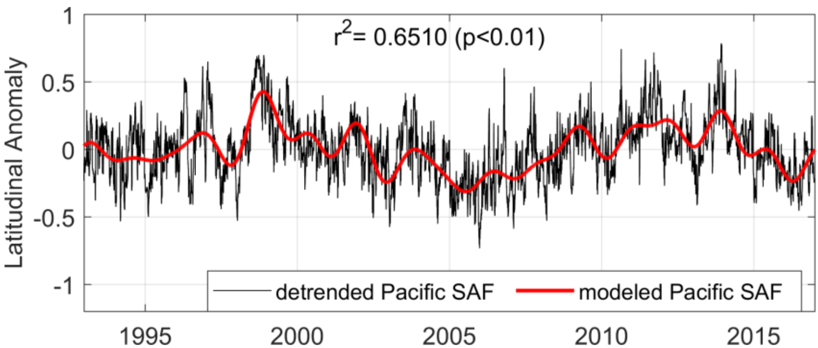

Figure 13. Daily Pacific SAF de-trended latitudinal anomaly and the reconstructed signal based on low-passed filtered series (red) for the period from 1993 to 2016. Pearson's correlation (r^2) and significance level (p) are displayed on top-center.

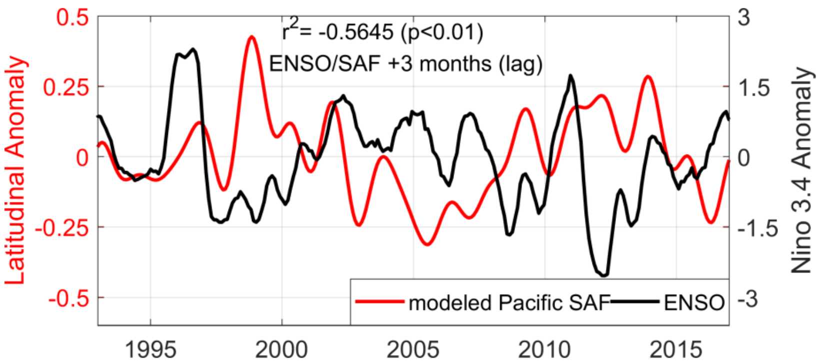

Figure 14. Pacific SAF (red) and ENSO (black) from 1993 to 2016. ENSO index is SST anomalies averaged within the NINO34 box (120°W – 170°W, 5°N – 5°S). Pearson's correlation (r^2) , significance level (p) and lag ratio are displayed on top-center.

Finally we perform a cross-correlation analysis between the TJS and SAF in each ocean basin. The maximum correlation occurs at zero lag and is +0.22 for the Atlantic, +0.17 for the Pacific and +0.21 for the Indian oceans. The coefficients are statistically significant, albeit weak. Climate change tends to push the TJS and SAF poleward and this can bee seen through the long-term trends presented here. However, the interannual variability (correlation analysis) shows they might vary independently. The winds change the ocean circulation but the jet position can be anchored by frontal oceanic systems (Sinclair, 1995; O'Reilly and Czaja, 2015), especially over open water regions. The mean SAF position of ~46°S for the Atlantic and Indian and ~54° for the Pacific reported here may play a role on the TJS location. The warming of Southern Ocean may be the key to understanding the poleward migration of SSH contours reported here (Hughes, 2000; Gille, 2008; Sutton and Roemmich, 2011). The higher temperatures increase the pressure difference between pole and mid-latitudes, intensifying the Southern Annular Mode (Thompson and Solomon, 2002). The warmer waters reach farther south, closer to Antarctic continent, increasing heat transport and promoting the basal melting and thinning of ice shelves in regions where the current is closer to the pole, i.e. the Amundsen and Bellingshausen seas (Pritchard et al. 2012; Paolo et al. 2015).

SUMMARY AND CONCLUSIONS

We used multiple datasets to investigate two large-scale circulation features of the Southern Hemisphere. The zonal wind velocity data between 700 and 925 hPa was used to track the TJS while temperature profiles from Argo floats and SSH from altimetry were used to identify the SAF. Both features were analyzed individually for the Atlantic, Pacific and Indian oceans.

The TJS presented a poleward migration and strengthening in the three oceans as previous studies has shown globally, particularly after 2000. The SAF also migrated poleward in the three oceans. This is consistent with warming of southern waters and the expansion of the tropical belt due to the increase of greenhouse gases and the cooling of the stratosphere due to ozone depletion, as suggested by previous works. The IPO and ENSO influence in the STJ and SAF position in the Pacific, pushing the both poleward during positive phases (El Niños) and equatorward during negative phases (La Niñas).

The future climate projections are expected to aggravate these trends and impact human life, by melting Antarctic ice, causing global sea level rising and coastal erosion (Church and White, 2011). The TJS and the ACC are key features to understand the Southern Hemisphere climate, although further research is required to discriminate the mechanisms that influence these features and their connection in future projections.

ACKNOWLEDGEMENTS

This work was supported by *Instituto Nacional de Ciências e Tecnologia para Mudanças Climáticas (INCT-MC Fase II)* Grant# 465501/2014-1 and by *Coordenação de Aperfeiçoamento de Pessoal de Nível Superior (CAPES)* Grant# 88887.136402/2017-00. This work is also part of the *Programa de Pós Graduação em Oceanografia (PPGOceano)* - *UFSC.*

REFERENCES

ARCHER, C. L. & CALDEIRA, K. 2008. Historical trends in the jet streams. *Geophysical Research Letters*, 35, 1–6.

ARGO GDAC (Argo float data and metadata from Global Data Assembly Centre). 2000. SEANOE.

ARGO DATA MANAGEMENT TEAM. 2017. *Argo User's Manual*. v.3.2. IFREMER

BELKIN, I. M. & GORDON, A. L. 1996. Southern Ocean fronts from the Greenwich meridian to Tasmania. *Journal of Geophysical Research*, 101, 3675–3696.

BELKIN, I. M. & REILLY, J. E. O. 2009. An algorithm for oceanic front detection in chlorophyll and SST satellite imagery. *Journal of Marine Systems*, 78, 319–326.

BENESTY, J., CHEN, J., HUANG, Y., & COHEN, I. 2009. Pearson Correlation Coefficient. *Noise Reduction in Speech Processing.* Springer Topics in Signal Processing. Vol 2. Springer, Berlin, Heidelberg.

DE BOER, A. M., GRAHAM, R. M., THOMAS, M. D. & KOHFELD, K. E. 2013. The control of the Southern Hemisphere Westerlies on the position of the subtropical front. *Journal of Geophysical Research: Oceans*, 118, 5669–5675.

BLUESTEIN, H.B., 1993. *Synoptic-Dynamic Meteorology in Midlatitudes. Vol. 2. Observations and Theory of Weather Systems.* Oxford University Press, Oxford.

BRACEWELL, R.N.,1966. The Fourier transform and its applications. *American Journal of Physics*, 34, 712-712.

CARLETON, A. M. 1979. A Synoptic Climatology of Satellite-Observed Extratropical Cyclone Activity for the Southern Hemisphere Winter. *Arch. Met. Geoph. Biokl. B.*, 279, 265–279.

CHAPMAN, C. C. 2014. Southern Ocean jets and how to find them: Improving and comparing common jet detection methods. *Journal of Geophysical Research: Oceans*, 119, 4318–4339.

CHATTERJEE, S., HADI, A., & PRICE, B. 2000. *Regression Analysis by Example.* Wiley VCH, New York.

CHURCH, J. A. & WHITE, N. J. 2011. Sea-Level Rise from the Late 19th to the Early 21st Century. *Surveys in Geophysics*, 32, 585–602.

CMEMS (Copernicus Marine Environment Monitoring System). 2018. *Product user manual*. V.4.

CUNNINGHAM, S. A., ALDERSON, S. G. & KING, B. A. 2003. Transport and variability of the Antarctic Circumpolar Current in Drake Passage. *Journal of Geophysical Research*, 108, 1–17.

DEE, D. P., UPPALA, S. M., SIMMONS, A. J., BERRISFORD, P., POLI, P., KOBAYASHI, S., ANDRAE, U., BALMASEDA, M. A., BALSAMO, G., BAUER, P., BECHTOLD, P., BELJAARS, A. C. M., BERG, L. Van De, BIDLOT, J., BORMANN, N., DELSOL, C., DRAGANI, R., FUENTES, M., GEER, A. J. & DEE, D. P. 2011. The ERA-Interim reanalysis : configuration and performance of the data assimilation system. *Quarterly Journal of the Royal Meteorological Society*, 137, 553–597.

DONG, S., SPRINTALL, J. & GILLE, S. T. 2006. Location of the Antarctic Polar Front from AMSR-E Satellite Sea Surface Temperature Measurements. *Journal of Physical Oceanography*, 36, 2075–2089.

DONOHUE, K. A., TRACEY, K. L., WATTS, D. R., CHIDICHIMO, M. P. & CHERESKIN, T. K. 2016. Mean Antarctic Circumpolar Current transport measured in Drake Passage. *Geophysical Research Letters*, 43, 761–767.

DUCHON, C. E. 1979. Lanczos Filtering in One and Two Dimensions. *Journal of applied meteorology*, 18, 1016–1022.

EICHELBERGER, S. J. & HARTMANN, D. L. 2007. Zonal jet structure and the leading mode of variability. *Journal of Climate*, 20, 5149–5163.

EMERY, W. J. 1977. Antarctic polar frontal zone from Australia to the Drake Passage. *Journal of Physical Oceanography*, 7, 811–822.

ENGLAND, M.H., MCGREGOR, S., SPENCE, P., MEEHL, G.A., TIMMERMANN, A., CAI, W., GUPTA, A.S., MCPHADEN, M.J., PURICH, A. & SANTOSO, A., 2014. Recent intensification of wind-driven circulation in the Pacific and the ongoing warming hiatus. *Nature Climate Change,* 4, 222.

FOFONOFF, P.N., & MILLARD, R. 1983. Algorithms for computation of fundamental properties of seawater. *Unesco Technical Papers in Marine Sciences*, 44, 53.

GIGLIO, D. & JOHNSON, G. C. 2015. Subantarctic and Polar fronts of the Antarctic Circumpolar Current and Southern Ocean heat and freshwater content variability: A view from Argo*. *Journal of Physical Oceanography*, 46, 749–768.

GILL, 1982. Atmosphere-Ocean Dynamics. *Quarter Journal of the Royal Meteorological Society*, 110, 280-281.

GILLE, S. T. 2008. Decadal-Scale Temperature Trends in the Southern Hemisphere Ocean. *American Meteorological Society*, 21, 4749–4765.

GILLE, S. T. 2014. Meridional displacement of the Antarctic Circumpolar Current. *Proceedings of the Royal Society*, 372, 20130273.

GOLUB, G. H. & REINSCH, C. 1970. Singular Value Decomposition and Least Squares Solutions. *Numerische Mathematik*, 14, 403–420.

GRAHAM, R. M., DE BOER, A. M., HEYWOOD, K. J., CHAPMAN, M. R. & STEVENS, D. P. 2012. Southern Ocean fronts: Controlled by wind or topography? *Journal of Geophysical Research: Oceans*, 117, 1–14.

GRAY, M.W., 1968. Global view of the origin of tropical disturbances and storms. *Monthly Weather Review,* 96, 669–700.

HANSEN, J., LACIS, a., RIND, D., RUSSELL, G., STONE, P., FUNG, I., RUEDY, R. & LERNER, J. 1984. Climate sensitivity: Analysis of feedback mechanisms. *Climate Processes and Climate Sensitivity (AGU Geophysical Monograph Series 29)*, 5, 130–163.

HOLTON, J.R., 1992. *An Introduction to Dynamic Meteorology*. Elsevier Academic Press. Burlington.

HU, Y. & FU, Q. 2007. and Physics Observed poleward expansion of the Hadley circulation since 1979. *Atmospheric Chemistry and Physics*, 7, 5229–5236.

HUGHES, L. 2000. Biological consequences of global warming: is the signal already. *Tree*, 15, 56–61.

KIM, Y. S. & ORSI, A. H. 2014. On the Variability of Antarctic Circumpolar Current Fronts Inferred from 1992–2011 Altimetry*. *Journal of Physical Oceanography*, 44, 3054–3071.

NAKAMURA, H. & SHIMPO, A. 2004. Seasonal variations in the Southern Hemisphere storm tracks and jet streams as revealed in a reanalysis dataset. *Journal of Climate*, 17, 1828–1844.

O'REILLY, C. H. & CZAJA, A. 2015. The response of the pacific storm track and atmospheric circulation to kuroshio extension variability. *Quarterly Journal of the Royal Meteorological Society*, 141, 52–66.

IHO (International Hidrographic Organization). 1953. *Limits of Ocean and Seas*. Vol. 28.

ORSI, H., WHITWORTH, T. & NOWLIN, W. D. J. 1995. On the meridional extent and fronts of the Antarctic Circumpolar Current. *Deep Sea Research*, 42, 641–673.

PAOLO, F., FRICKER, H. A. & PADMAN, L. 2015. Ice sheets. Volume loss from Antarctic ice shelves is accelerating. *Science*, 348, 327–331.

POLVANI, L.M., SOBEL, A.H., & WAUGH, D.W., 2013. *The stratosphere: dynamics, transport, and chemistry*. American Geophysical Union.

POLVANI, L. M., WAUGH, D. W., CORREA, G. J. P. & SON, S. 2011. Stratospheric Ozone Depletion: The Main Driver of Twentieth-Century Atmospheric Circulation Changes in the Southern Hemisphere. *American Meteorological Society*, 24, 795–812.

PRITCHARD, H. D., LIGTENBERG, S. R. M., FRICKER, H. a., VAUGHAN, D. G., VAN DEN BROEKE, M. R. & PADMAN, L. 2012. Antarctic ice-sheet loss driven by basal melting of ice shelves. *Nature*, 484, 502–505.

RANDEL, W. J. & WU, F. 1999. Cooling of the Arctic and Antarctic Polar Stratospheres due to Ozone Depletion. *American Meteorological Society*, 12, 1467–1479.

ROEMMICH, D. & GILSON, J. 2009. The 2004 – 2008 mean and annual cycle of temperature , salinity , and steric height in the global ocean from the Argo Program. *Progress in Oceanography*, 82, 81–100.

SALLÉE, J. B., SPEER, K. & MORROW, R. 2008. Response of the antarctic circumpolar current to atmospheric variability. *Journal of Climate*, 21, 3020–3039.

SINCLAIR, M. R. 1995. A climatology of Cyclogenesis for the Southern Hemisphere. *Monthly Weather Review*, 123, 1601–1619.

SOKOLOV, S. & RINTOUL, S. R. 2007. Multiple Jets of the Antarctic Circumpolar Current South of Australia*. *Journal of Physical Oceanography*, 37, 1394–1412.

SOKOLOV, S. & RINTOUL, S. R. 2009*a*. Circumpolar structure and distribution of the antarctic circumpolar current fronts: 2. Variability and relationship to sea surface height. *Journal of Geophysical Research: Oceans*, 114, 1–15.

SOKOLOV, S. & RINTOUL, S. R. 2009*b*. Circumpolar structure and distribution of the antarctic circumpolar current fronts: 1. Mean98 circumpolar paths. *Journal of Geophysical Research: Oceans*, 114, 1–19.

SUN, C. & WATTS, D. R. 2002. A view of ACC fronts in streamfunction space. *Deep Sea Research Part A, Oceanographic Research Papers*, 49, 1141–1164.

SUTTON, P. & ROEMMICH, D. 2011. Decadal steric and sea surface height changes in the Southern Hemisphere. *Geophysical Research Letters*, 38, 4–7.

SWART, N. C., FYFE, J. C., 2012. Observed and simulated changes in the Southern Hemisphere surface westerly wind-stress. *Geophysical Research Letters*, 39, L16711.

THOMPSON, A. F. & SALLEE, J.-B. 2012. Jets and topography: jet transitions and the impact on transport in the Antarctic Circumpolar Current. *Journal of Physical Oceanography*, 42, 956–972.

THOMPSON, D. W. J. & SOLOMON, S. 2002. Interpretation of Recent Southern Hemisphere Climate Change. *Science*, 296, 895899.

TOGGWEILER, J. R. & RUSSELL, J. L. 2008. Ocean circulation in a warming climate. *Nature*, 451, 286–288.

TRENBERTH, K. E. 1991. StormTracks in the Southern Hemisphere. *Journal of Atmospheric Sciences*, 48, 2159–2178.

TRENBERTH, K. E. & STEPANIAK, D. P. 2001. Indices of El Nino Evolution. *Journal of Climate*, 14, 1697–1701.

TRENBERTH, K. E., LARGE, W. G. & OLSON, J. G. 1990. The Mean Annual Cycle in Global Ocean Wind Stress. *Journal of Physical Oceanography*, 20, 1742–1760.

TRULL, T., RINTOUL, S. R., HADFIELD, M. & ABRAHAM, E. R. 2001. Circulation and seasonal evolution of polar waters south of Australia: Implications for iron fertilization of the Southern Ocean. *Deep-Sea Research Part II: Topical Studies in Oceanography*, 48, 2439–2466.

VECCHI, G.A., & SODEN, B.J. 2007. Increased tropical Atlantic wind shear in model projections of global warming. *Geophysical Research Letters*, 34, L08702.

WHITWORTH, T., NOWLIN JR, W. D. & WORLEY, S. J. 1982. The net transport of the Antarctic Circumpolar Current through Drake Passage. *Journal of Physical Oceanography*, 12, 960–971.

WOOLLINGS, T., HANNACHI, A. & HOSKINS, B. 2010. Variability of the North Atlantic eddy-driven jet stream. *Quarterly Journal of the Royal Meteorological Society*, 136, 856–868.

CONCLUSÕES E CONSIDERAÇÕES FINAIS

Múltiplos bancos de dados foram utilizados para investigar as principais feições dinâmicas da circulação de larga escala no Hemisfério Sul. A velocidade zonal do vento entre 700 e 925 hPa foi usada para encontrar o JT enquanto perfis de temperatura de flutuadores Argo e ASM de altímetros foram usados para identificar a FSA. Tanto o JT quanto a FSA foram analisados individualmente nos Oceanos Atlântico, Pacífico e Índico.

O JT apresentou uma migração em direção ao polo e teve um aumento de velocidade em escala global, particularmente após os anos 2000, como tem sido mostrado em estudos anteriores. A série de dados do jato mostrou uma grande variação latitudinal, oscilando entre 40°S e 60°S com posições medias de ~50°S nos Oceanos Atlântico e Índico, e ~55°S no Oceano Pacífico.

A ASM capturou satisfatoriamente a posição da FSA, pois a mesma está em concordância com um número significativo de outros estudos no assunto (Orsi et al. 1995; Belkin and Gordon, 1996; Sokolov and Rintoul, 2009a,b; Gille, 2014; Kim & Orsi, 2014), como mostra a figura 5.

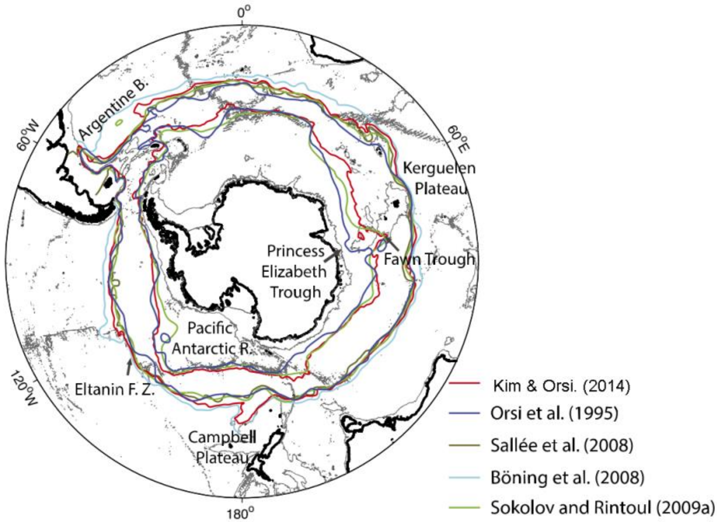

Fonte: Kim & Orsi, 2014

Figura 5. Posição geográfica da FSA e da FP de acordo com diversos estudos.

A FSA também migrou para o polo nos três oceanos. Este resultado é consistente com o aquecimento das águas austrais e expansão do cinturão tropical devido ao aumento dos gases de efeito estufa e ao resfriamento da estratosfera pela depleção de ozônio, como sugerem trabalhos prévios. Essa migração não é acompanhada pelo fluxo principal da corrente, restringindo-se a um deslocamento nas propriedades da água. No entanto a migração de águas com diferentes concentrações de nutrientes tem impacto nas espécies que habitam a região e está ligada a fenômenos climáticos globais.

O ENSO mostrou ter influência sobre a posição da FSA no Oceano Pacífico com uma correlação inversa. Em fases positivas de El Niño, o aquecimento das águas do Pacífico Tropical empurra os contornos de ASM para sul, enquanto em anos de La Niña as águas frias trazem a FSA para norte. Foi constatado que as correlações máximas ocorrem quando o ENSO lidera a posição da FSA no Pacífico por 3 meses, possivelmente devido à lenta resposta do oceano a mudanças atmosféricas.

As futuras projeções do clima esperam um agravamento dessas tendências e um aumento do impacto na vida humana, através do derretimento de gelo Antártico, aumento do nível global dos oceanos e consequentemente da erosão costeira. (Church and White, 2011).O JT e a CCA são peças-chave no entendimento do clima do Hemisfério Sul, apesar de que pesquisas adicionais serão necessárias para discriminar os mecanismos que influenciam essas feições e sua conexão nessas futuras projeções.

REFERÊNCIAS

ALVAIN, S., MOULIN, C., DANDONNEAU, Y., & LOISEL, H. Seasonal distribution and succession of dominant phytoplankton groups in .... **Global Geochemiclal Cycles**, v. *22*(September). 2008. Disponível em <https://doi.org/10.1029/2007GB003154

BELKIN, I. M. & GORDON, A. L. 1996. Southern Ocean fronts from the Greenwich meridian to Tasmania. **Journal of Geophysical Research,** 101, 3675–3696.

BELKIN, I. M. & REILLY, J. E. O. 2009. An algorithm for oceanic front detection in chlorophyll and SST satellite imagery. **Journal of Marine Systems**, 78, 319–326.

BLUESTEIN, H.B., 1993. Synoptic-Dynamic Meteorology in Midlatitudes. Vol. 2. Observations and Theory of Weather Systems. **Oxford University Press,** Oxford.

DE BOER, A. M., GRAHAM, R. M., THOMAS, M. D. & KOHFELD, K. E. 2013. The control of the Southern Hemisphere Westerlies on the position of the subtropical front. **Journal of Geophysical Research: Oceans**, 118, 5669–5675.

BROEKER, W. S. The Great Ocean Conveyor. **Oceanography.** v. 4(2). 1991.

BYRNE, K. What is El Niño? **AccuWeather. New York, N.C. 2**019. Retrieved from https://www.accuweather.com/en/weather-news/what-is-el-nino/70005474>.

BUSTAMANTE, R., COLOMA, L. A., CONSUEGRA, J. A., FOGDEN, M. P. L., POUNDS, J. A., PUSCHENDORF, R., … SA, G. A. Widespread amphibian extinctions from epidemic disease driven by global warming, v. *439*(January), p. 161–167. 2006. Disponível em <https://doi.org/10.1038/nature04246>.

CHURCH, J. A. & WHITE, N. J. Sea-Level Rise from the Late 19th to the Early 21st Century. **Surveys in Geophysics**, 32, 585–602. 2011.

CUNNINGHAM, S. A., ALDERSON, S. G. & KING, B. A. 2003. Transport and variability of the Antarctic Circumpolar Current in Drake Passage. **Journal of Geophysical Research,** 108, 1–17.

DONG, S., SPRINTALL, J. & GILLE, S. T. 2006. Location of the Antarctic Polar Front from AMSR-E Satellite Sea Surface Temperature Measurements. *Journal of Physical Oceanography*, 36, 2075–2089.

DONOHUE, K. A., TRACEY, K. L., WATTS, D. R., CHIDICHIMO, M. P. & CHERESKIN, T. K. 2016. Mean Antarctic Circumpolar Current transport measured in Drake Passage. **Geophysical Research Letters,** 43, 761–767.

EICHELBERGER, S. J. & HARTMANN, D. L. 2007. Zonal jet structure and the leading mode of variability. *Journal of Climate*, 20, 5149–5163.

EMERY, W. J. 1977. Antarctic polar frontal zone from Australia to the Drake Passage. *Journal of Physical Oceanography,* 7, 811–822

GIGLIO, D. & JOHNSON, G. C. 2015. Subantarctic and Polar fronts of the Antarctic Circumpolar Current and Southern Ocean heat and freshwater content variability: A view from Argo*. **Journal of Physical Oceanography**, 46, 749–768.

GILL, 1982. Atmosphere-Ocean Dynamics. **Quarter Journal of the Royal Meteorological Society,** 110, 280-281.

GILLE, S. T. 2014. Meridional displacement of the Antarctic Circumpolar Current. **Proceedings of the Royal Society**, 372, 20130273.

GRAHAM, R. M., DE BOER, A. M., HEYWOOD, K. J., CHAPMAN, M. R. & STEVENS, D. P. 2012. Southern Ocean fronts: Controlled by wind or topography? **Journal of Geophysical Research: Oceans, 1**17, 1–14.

GRAY, M.W., 1968. Global view of the origin of tropical disturbances and storms. **Monthly Weather Review,** 96, 669–700.

HANSEN, J., LACIS, a., RIND, D., RUSSELL, G., STONE, P., FUNG, I., RUEDY, R. & LERNER, J. 1984. Climate sensitivity: Analysis of feedback mechanisms. **Climate Processes and Climate Sensitivity (AGU Geophysical Monograph Series 29)**, 5, 130–163.

HOLTON, J.R., 1992. An Introduction to Dynamic Meteorology. **Elsevier Academic Press.** Burlington.

HOUGHTON, J. T., DING, Y. D. J. G., GRIGGS, D. J., NOGUER, M., VAN DER LINDEN, P. J., XIAOSU, D., MASKELL, K. & JOHNSON, C. A. Climate change 2001: the scientific basis. **The Press Syndicate of the University of Cambridge**, 2001.

HU, Y. & FU, Q. 2007. and Physics Observed poleward expansion of the Hadley circulation since 1979. **Atmospheric Chemistry and Physics,** 7, 5229–5236.

IHO (International Hidrographic Organization). 1953. **Limits of Ocean and Seas**. Vol. 28.

KIM, Y. S. & ORSI, A. H. 2014. On the Variability of Antarctic Circumpolar Current Fronts Inferred from 1992–2011 Altimetry*. **Journal of Physical Oceanography**, 44, 3054–3071.

NATIONAL RESEARCH CONCIL. Future Science opportunities in Antarctica and the Southern Ocean. **The National Academies Press, Washington, D. C**. 2011

NIILER, P. P., MAXIMENKO, N. A., & MCWILLIAMS, J. C. Dynamically balanced absolute sea level of the global ocean derived from near-surface velocity observations. **Geophysical Research Letters**, v. 30(22), p. 3–6. 2003. Disponível em <https://doi.org/10.1029/2003GL018628>.

ORSI, A. H, & WHITWORTH, T. Hydrographic Atlas of the World Ocean Circulation Experiment (WOCE) Volume 1: Southern Ocean. 2005. Retrieved from https://escholarship.org/uc/item/3xh7d30p

ORSI, H., WHITWORTH, T. & NOWLIN, W. D. J. 1995. On the meridional extent and fronts of the Antarctic Circumpolar Current. **Deep Sea Research**, 42, 641–673.

PENG, S., HUANG, J., SHEEHY, J. E., LAZA, R. C., VISPERAS, R. M., ZHONG, X., CASSMAN, K. G. Rice yields decline with higher night temperature from global warming. **PROCEEDINGS OF THE NATIONAL ACADEMY OF SCIENCES OF THE UNITED STATES OF AMERICA**, v. *101*(27), p. 9971–9975. 2004.

POLVANI, L.M., SOBEL, A.H., & WAUGH, D.W., 2013. The stratosphere: dynamics, transport, and chemistry. **American Geophysical Union.**

POLVANI, L. M., WAUGH, D. W., CORREA, G. J. P. & SON, S. 2011. Stratospheric Ozone Depletion: The Main Driver of Twentieth-Century Atmospheric Circulation Changes in the Southern Hemisphere. **American Meteorological Society**, 24, 795–812.

PRITCHARD, H. D., LIGTENBERG, S. R. M., FRICKER, H. a., VAUGHAN, D. G., VAN DEN BROEKE, M. R. & PADMAN, L. 2012. Antarctic ice-sheet loss driven by basal melting of ice shelves**. Nature**, 484, 502–505.

RANDEL, W. J. & WU, F. 1999. Cooling of the Arctic and Antarctic Polar Stratospheres due to Ozone Depletion. **American Meteorological Society,** 12, 1467–1479.

ROEMMICH, D. & GILSON, J. The 2004 – 2008 mean and annual cycle of temperature , salinity , and steric height in the global ocean from the Argo Program. **Progress in Oceanograph**y, 82, 81–100. 2009.

SOKOLOV, S. & RINTOUL, S. R. 2007. Multiple Jets of the Antarctic Circumpolar Current South of Australia*. **Journal of Physical Oceanography**, 37, 1394–1412.

SOKOLOV, S. & RINTOUL, S. R. 2009*a*. Circumpolar structure and distribution of the antarctic circumpolar current fronts: 2. Variability and relationship to sea surface height. **Journal of Geophysical Research: Oceans,** 114, 1–15.

SOKOLOV, S. & RINTOUL, S. R. 2009*b*. Circumpolar structure and distribution of the antarctic circumpolar current fronts: 1. Mean98 circumpolar paths. **Journal of Geophysical Research: Oceans,** 114, 1–19.

SWART, N. C., FYFE, J. C., 2012. Observed and simulated changes in the Southern Hemisphere surface westerly wind-stress. **Geophysical Research Letters**, 39, L16711.

TOGGWEILER, J. R. & RUSSELL, J. L. 2008. Ocean circulation in a warming climate. **Nature,** 451, 286–288.

TRENBERTH, K. E., LARGE, W. G. & OLSON, J. G. 1990. The Mean Annual Cycle in Global Ocean Wind Stress. **Journal of Physical Oceanography,** 20, 1742–1760.

TRULL, T., RINTOUL, S. R., HADFIELD, M. & ABRAHAM, E. R. 2001. Circulation and seasonal evolution of polar waters south of Australia: Implications for iron fertilization of the Southern Ocean. **Deep-Sea Research Part II: Topical Studies in Oceanography,** 48, 2439–2466.

VECCHI, G.A., & SODEN, B.J. 2007. Increased tropical Atlantic wind shear in model projections of global warming. **Geophysical Research Letters**, 34, L08702.

WHITWORTH, T., NOWLIN JR, W. D. & WORLEY, S. J. 1982. The net transport of the Antarctic Circumpolar Current through Drake Passage. **Journal of Physical Oceanography,** 12, 960–971.